New Charge Transporting Host Material for Short Wavelength Organic Electrophosphorescence: 2,7-Bis(diphenylphosphine oxide)-9,9-dimethylfluorene

Asanga B. Padmaperuma, Linda S. Sapochak,* and Paul E. Burrows

Materials Division, Energy Science and Technology Directorate, Pacific Northwest National Laboratory, 908 Battelle Boulevard, Richland, Washington 99352

Received January 10, 2006. Revised Manuscript Received February 20, 2006

We report the synthesis, crystal structure, and photophysical and electroluminescent properties of a new charge transporting host material for short wavelength phosphor-doped organic light emitting devices (OLEDs) based on 2,7-bis(diphenylphosphine oxide)-9,9-dimethylfluorene (PO6). The P═O moiety is used as a point of saturation between the fluorene bridge and the outer phenyl groups so that the triplet exciton energy of PO6 is 2.72 eV, similar to that of a dibromo substituted fluorene, but it is more amenable to vacuum sublimation and has good film forming properties. Computational analysis (B3LYP/6-31G*) predicts the highest occupied molecular orbital and lowest unoccupied molecular orbital energies of PO6 to be lower by 1.5 and 0.59 eV, respectively, compared to a similar diphenylamino substituted derivative. In a simple bilayer OLED device, PO6 exhibits structured UV electroluminescence at a peak wavelength of 335 nm and structured lower energy emission with peaks at 380 and 397 nm, similar to the solid film and crystalline solid photoluminescence spectra. The longer wavelength peaks are attributed to aggregate formation via strong intermolecular interactions (P—O···H—C and edge-to-face C—H···π contacts) and longer range electrostatic interactions between P═O moieties leading to ordered regions in the film. Devices incorporating PO6 as the host material doped with iridium(III)bis(4,6-(difluorophenyl)pyridinato-*N*,*C*2)picolinate (FIrpic) exhibited sky blue emission with peak external quantum efficiency ($\eta_{ext,max}$) of 8.1% and luminous power efficiency ($\eta_{p,max}$) of 25.1 lm/W. At a brightness of 800 cd/m^2, generally considered to be sufficient for lighting applications, the η_{ext} and η_p are 6.7% and 11.8 lm/W and the operating voltage is 5.6 V, which is significantly lower than has been demonstrated previously using this dopant.

Introduction

The synthetic versatility of organic materials allows the optimization of their physical properties including emission energy, charge transport, and morphological stability which are all important for efficient organic light emitting device (OLED) operation.[1,2] Improvements in OLED performance over the past decade have resulted in commercially available products.[3] Organometallic small molecule phosphor-doped OLEDs have demonstrated by far the highest quantum efficiency (QE) with >90% internal QE demonstrated in green pixels.[4] Operating voltages of small molecules, however, remain high (typically ∼ 10 V at high brightness) compared to polymer-based OLEDs unless ionic or small molecule dopants are added.[5] Long-lived blue phosphorescent OLEDs have yet to be demonstrated, in part because of the lack of appropriate organic charge transport materials into which to dope the phosphorescent emitter. Blue electrophosphorescence is a particular challenge because the triplet excited state of the host material must be higher than that of the dopant to prevent quenching of the dopant emission.[6]

Typically, organometallic phosphors are physically doped into a conductive host matrix, and electroluminescence (EL) from the dopant results from energy transfer from the host and/or direct trapping of charge on the phosphor.[7,8] The charge transporting host material for a blue OLED must exhibit triplet level emission <450 nm which requires an extremely limited conjugation length. It is difficult to meet these requirements because there is a tradeoff between increasing the band gap of the material to increase singlet and triplet energies and decreasing the π-aromatic system, which may adversely affect charge transport properties. Deeper blue phosphors have been demonstrated using insulating, wide band gap host materials with charge transport occurring via hopping between adjacent dopant molecules,[8] but this leads to increased operating voltage and, therefore, less power efficient devices. Furthermore, there is concern that forcing charge transport (i.e., repeated oxidation and

* Corresponding author. E-mail: linda.sapochak@pnl.gov. Tel.: 509 375-6942. Fax: 509 375-2186.

(1) The Special Issue on Organic Electronics. *Chem. Mater.* **2004**, *16*, 4381−4846.
(2) Mitschke, U.; Bauerle, P. *J. Mater. Chem.* **2000**, *10*, 1471. Kalinowski, J. *J. Phys. D: Appl. Phys.* **1999**, *32*, R179.
(3) Howard, W. E. Better Displays with Organic Films. *Sci. Am.* **2004**.
(4) Adachi, C.; Baldo, M.; Thompson, M. E.; Forrest, S. R. *J. Appl. Phys.* **2001**, *90*, 5048.
(5) Pfeiffer, M.; Leo, K.; Zhou, X.; Huang, J. S.; Hofmann, M.; Werner, A.; Blochwitz-Nimoth, J. *Org. Elect.* **2003**, *4*, 89.
(6) Adachi, C.; Kwong, R.; Djurovich, P.; Adamovich, V.; Baldo, M. A.; Thompson, M. E.; Forrest, S. R. *Appl. Phys. Lett.* **2001**, *79*, 2082.
(7) Holmes, R. J.; Forrest, S. R.; Tung, Y. J.; Kwong, R. C.; Brown, J. J.; Garon, S.; Thompson, M. E. *Appl. Phys. Lett.* **2003**, *82*, 2422.
(8) Holmes, R. J.; D'Andrade, B. W.; Forrest, S. R.; Ren, X.; Li, J.; Thompson, M. E. *Appl. Phys. Lett.* **2003**, *83*, 3818.

10.1021/cm0600677 CCC: $33.50
Published on Web 03/31/2006

reduction) onto the light emitting dopant may compromise long-term stability.

We recently reported that 4,4′-bis(diphenylphosphine oxide)biphenyl (PO1) serves as a wide band gap and charge transporting host material for iridium(III)bis(4,6-(difluorophenyl)pyridinato-*N*,*C*2)picolinate (FIrpic) in electrophosphorescent devices with a peak QE of 7.8% and low drive voltage.[9] The P═O groups act as points of saturation between the "active" biphenyl chromophore bridge and the outer, higher energy phenyl groups. In this way, a high triplet state biphenyl bridge is used as a building block to construct a larger molecule with physical properties amenable to device fabrication without compromising the desired photophysical properties of biphenyl. In this paper, we extend this technique to use a 9,9-dimethylfluorene (DMeF) bridging group.

Fluorene-based polymers and oligomers have been used as electronic materials because of their good thermal and chemical stability along with high emission efficiencies.[10] However, most fluorene derivatives have relatively low-lying triplet exciton levels and indeed usually suffer from low energy singlet emission attributed to excimer, aggregate, or ketonic defects.[11] They are, therefore, unsuitable as high energy host materials. Here, we create a new fluorene derivative capable of serving as a charge transporting host for a short wavelength electrophosphorescent dopant by substituting the fluorene chromophore with diphenylphosphine oxide moieties resulting in 2,7-bis(diphenylphosphine oxide)-9,9-dimethylfluorene (PO6). The synthesis and characterization of this new fluorene derivative, including crystal structure and photophysical and EL properties, are presented.

Experimental Section

Synthesis and Characterization. All chemicals used in synthetic procedures were obtained from Aldrich Chemical Co. and used as received unless noted otherwise. 2,7-Dibromo-9,9-dimethylfluorene (BrDMeF) was prepared and purified according to published procedures.[12] Synthesis of 2,7-bis(diphenylphosphine oxide)-9,9-dimethylfluorene (PO6) was accomplished by a modified literature procedure outlined in Scheme 1.[13] A lithium−halogen exchange reaction between BrDMeF and *n*-butyllithium followed by reaction with chlorodiphenylphosphine gave crude 2,7-bis(diphenylphosphine)-9,9-dimethylfluorene (P6), which was isolated and chromatographed before being oxidized with 30% H_2O_2 to give PO6. The diphosphine oxide was first purified by column chromatography followed by multiple sublimations via high vacuum, gradient temperature sublimation. The chemically pure material was heated incrementally in zone 1 of a three-zone furnace from 100 to 260

Scheme 1

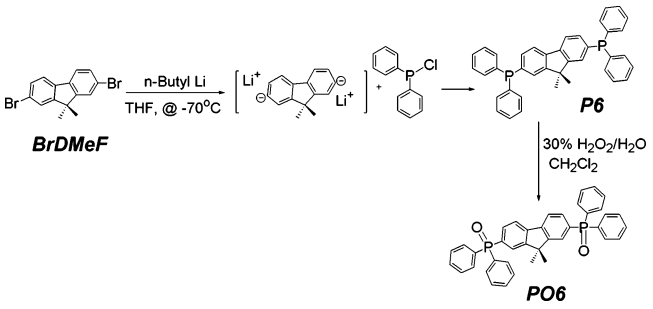

°C over a period of 3 days. During the first sublimation process, diphosphine and monophosphine oxide impurities were sublimed (85−175 °C at ∼10^{-6} Torr) and separated (confirmed by thin layer chromatography) from PO6, which sublimed at ∼260 °C (∼10^{-6} Torr). This material was purified in this manner twice more to provide pure PO6 which sublimed at ∼275 °C (10^{-6} Torr).

Thermal analysis by differential scanning calorimetry (DSC) using a Netzsch simultaneous thermal analyzer (STA400) was performed to determine melting point and glass forming properties. Sublimed samples (∼5 mg) were placed in aluminum pans and heated at 20 °C/min under N_2 gas at a flow rate of 50 mL/min. Indium metal was used as the temperature standard. During the first heating cycle, PO6 exhibited a single endothermic melting transition at 287 °C. After quenching the melted sample in liquid nitrogen, the second heating revealed a glass transition (T_g = 105 °C) and crystallization exotherm (T_{c1} onset = 206 °C) followed by melting again at 287 °C. In contrast, the dibromo derivative, BrDMeF, melts at 181 °C and does not form a glass under similar experimental conditions.

NMR spectra were obtained using a Varian Infinity CMX 300-MHz NMR spectrometer at the following frequencies: 300 MHz (^{1}H), 121.4 MHz (^{31}P), and 100.6 MHz (^{13}C). Tetramethylsilane was used as an internal reference for ^{1}H and ^{13}C spectra, and the ^{31}P signals were externally referenced to 85% H_3PO_4. Elemental analysis was performed by Desert Analytics Laboratories, Tucson, AZ, U.S.A.

2,7-Bis(diphenylphosphine)-9,9-dimethylfluorene (P6). A total of 5.0 g [0.0142 mol] of BrDMeF was dissolved in 100 mL of anhydrous tetrahydrofuran under argon and cooled to ∼−70 °C (dry ice: IPA bath). A total of 2.1 equiv of *n*-butyllithium [2.5 M in hexanes] was added slowly dropwise to give a bright yellow solution that thickened to a slurry. The temperature was not allowed to rise above −60 °C during the addition. Stirring was continued for 3 h at −70 °C after which 5.3 mL [0.0284 mol] of chlorodiphenylphosphine was added giving a clear, pale yellow solution. The reaction was stirred for 3 h more at −70 °C before quenching with 2 mL of degassed methanol. Volatiles were removed under a reduced pressure to give an off-white solid that was digested in methanol, filtered, then digested in water, and filtered. The crude material was purified by column chromatography (R_f = 0.39, SiO_2, ethyl acetate/hexanes = 1:9) to give 5.70 g (71%) of chemically pure P6. Mp: 193 °C (DSC, 20 K/min, N_2). ^{1}H NMR ($CDCl_3$, 295 K): δ 7.62 (d, 2H), 7.44 (d, 2H), 7.3−7.4 (24H), 7.21 (t, 2H), 1.37 (s, 6H). ^{31}P NMR $CDCl_3$, 295 K): δ −3.52.

2,7-Bis(diphenylphosphine oxide)-9,9-dimethylfluorene (PO6). A total of 5.70 g [0.01 mol] of P6, 50 mL of methylene chloride, and 10 mL of 30% hydrogen peroxide were stirred overnight at room temperature. The organic layer was separated and washed with water and then brine. The extract was evaporated to dryness affording a white solid, which was further purified by column chromatography (R_f = 0.72, SiO_2, ethyl acetate/hexanes/methanol = 2:2:1) to yield 5.72 g (95%) of chemically pure PO6. Mp: 287 °C (DSC, 20

(9) Burrows, P. E.; Padmaperuma, A. B.; Sapochak, L. S.; Djurovich, P.; Thompson, M. E. *Appl. Phys. Lett.* **2006**, in press.
(10) Neher, D. *Macromol. Rapid Commun.* **2001**, *22*, 1365. Scherf, U.; List, E. J. W. *Adv. Mater.* **2002**, *14*, 477.
(11) For further examples see these papers and the references therein: Sims, M.; Bradley, D. D. C.; Ariu, M.; Koeberg, M.; Asimakis, A.; Grell, M.; Lidzey, D. G. *Adv. Funct. Mater.* **2004**, *14*, 765. Lim, S. F.; Friend, R. H.; Rees, I. D.; Li, J.; Ma, Y. G.; Robinson, K.; Holmes, A. B.; Hennebicq, E.; Beljonne, D.; Cacialli, F. *Adv. Funct. Mater.* **2005**, *15*, 981. List, E. J. W.; Guntner, R.; de Freitas, P. S.; Scherf, U. *Adv. Mater.* **2002**, *14*, 374. Yang, X. H.; Jaiser, F.; Neher, D.; Lawson, P. V.; Brèdas, J. L.; Zojer, E.; Guntner, R.; de Freitas, P. S.; Forster, M.; Scherf, U. *Adv. Funct. Mater.* **2004**, *14*, 1097.
(12) Saroja, G.; Zhang, P.; Nikolaus, P. E.; Liebscher, J. *J. Org. Chem.* **2004**, *69*, 987. Belfield, K. D.; Schafer, K. J.; Mourad, W.; Reinhardt, B. A. *J. Org. Chem.* **2000**, *65*, 4475.
(13) Baldwin, R. A.; Cheng, M. T. *J. Org. Chem.* **1967**, *32*, 1572.

K/min, N_2). ^{1}H NMR ($CDCl_3$, 295 K): δ 7.94 (d, 2H, J = 11.8 Hz), 7.79 (dd, 2H, J = 2.2 Hz, 7.8 Hz), 7.72 (m, 8H), 7.55 (m, 4H), 7.46−7.52 (m, 8H), 1.37 (s, 6H). ^{13}C NMR ($CDCl_3$, 295 K): δ 154.4, 141.5, 132.9, 132.5, 132.1, 132.0, 131.9, 131.7, 131.2, 45.4, 26.6. ^{31}P NMR ($CDCl_3$, 295 K): δ 31.2. Anal. Calcd for $C_{39}H_{32}P_2O_2$: C, 78.78; H, 5.42; P, 10.42. Found: C, 78.78; H, 5.61; P, 10.00.

X-ray Crystallographic Characterization. Colorless prismatic crystals of PO6 suitable for single-crystal X-ray diffraction were obtained from recrystallization of the sublimed material from a CH_2Cl_2/hexane solution. The crystals were selected under ambient conditions, coated in epoxy, and mounted on the end of a glass fiber. Crystal data collection was performed on a Bruker CCD-1000 diffractometer with Mo Kα (λ = 0.710 73 Å) radiation and a collector-to-crystal distance of 5.03 cm. Cell constants were determined from a list of reflections found by an automated search routine. Data were collected using the full sphere routine and were corrected for Lorentz and polarization effects. The absorption corrections were based on fitting a function to the empirical transmission surface as sampled by multiple equivalent measurements using SADABS software.[14] Positions of the heavy atoms were found by the Patterson method. The remaining atoms were located in an alternating series of least-squares cycles and difference Fourier maps. All non-hydrogen atoms were refined in full-matrix anisotropic approximation. All hydrogen atoms were placed in the structure factor calculation at idealized positions and refined using a riding model. Complete data collection and reduction information can be found in Supporting Information.

Computational Methods. Electronic structure calculations were performed with Spartan '04 (Version 1.0.3; Wavefunction, Inc.) at the B3LYP/6-31G* level. The highest occupied molecular orbital (HOMO) and lowest unoccupied molecular orbital (LUMO) energies were determined from the minimized singlet geometry to approximate the ground-state molecule. The starting geometry for PO6 was obtained from the X-ray crystal structure.

Photophysical Characterization. Absorbance spectra were recorded with a Shimadzu UV-2501PC ultraviolet−visible dual-beam spectrometer. Steady-state emission spectra were recorded at room temperature using a Jobin-Yvon SPEX Fluorolog 2 (450-W Xe lamp). The fluorescence quantum yield was determined in dilute CH_2Cl_2 solution (optical density $\sim$ 0.1) according to the method described by Demas and Crosby[15] using quinine sulfate in 1.0 N H_2SO_4 (Q_R = 0.546)[16] as a reference. Singlet lifetime was determined in CH_2Cl_2 by exciting with the output of a frequency-doubled picosecond dye laser pumped by the second harmonic of a mode-locked Nd:vanadate laser operating at 76 MHz. The second harmonic at 280 nm was directed onto the sample, and light emission was collected at right angles and focused into a 1/8 m subtractive double monochromator equipped with a microchannel plate photomultiplier tube (PMT) operating in pulse-counting mode. The output of the PMT was sent into a standard time-correlated photon counting apparatus that produced a histogram of the number of photons versus photon arrival time. The time resolution of the apparatus was measured to be 50 ps full width at half-maximum using a standard scattering material.

Phosphorescence spectra were obtained in CH_2Cl_2 at 77 K at an excitation wavelength of 280 nm and time delay of 300 μs using a nanosecond optical parametric oscillator/amplifier operating at a 10 Hz repetition rate. The output was directed onto the sample, and emission was collected at right angles to the excitation and focused into a 1/8 m monochromator with a gated intensified charge-coupled device (CCD) camera to record the spectra. The gate of the CCD camera could be set to reject scattered laser light and short-lived luminescence, allowing the observation of long-lived luminescence.

EL Characterization. Organic chemicals used for fabricating devices were purified by high-vacuum, gradient-temperature sublimation, including PO6, FIrpic (purchased from American Dye Source), and copper phthalocyanine (CuPc, purchased from Aldrich). The hole transporting materials, *N*,*N*′-diphenyl-*N*,*N*′-bis(1-naphthol)-1,1′-biphenyl-4,4′-diamine (α-NPD) and 4,4′,4″-tris(carbazol-9-yl)triphenylamine (TCTA, purchased from H. W. Sands Corp.), were obtained as device-grade and used without further purification.

Devices were grown on glass slides precoated with indium tin oxide (ITO) with a sheet resistance of 15 Ω/square. The ITO substrates were cleaned as described previously[17] and exposed to UV-ozone for 10 min before being loaded into a nitrogen glovebox (<1 ppm H_2O, <0.5 ppm O_2) coupled to a multichamber vacuum deposition system. Organic layers were sequentially deposited by thermal evaporation from Ta boats in a vacuum chamber with base pressure < 10^{-7} Torr. Cathodes were defined by depositing a 1 nm thick layer of LiF immediately followed by a 100 nm thick layer of Al through a shadow mask with 1 mm diameter circular openings. A quartz crystal oscillator placed near the substrate was used to measure the thicknesses of the films, which were calibrated ex situ using ellipsometry. Devices were tested in air with electrical contact made using a W probe tip on the ITO anode and a 0.002 in. diameter Au wire probe directly on the Al cathode. Current−voltage characteristics were measured with an Agilent Technologies 4155B semiconductor parameter analyzer. Light output was measured using a 1 cm^2 Si photodetector placed behind the OLED. No corrections are made for light waveguided in the organic thin films or the substrate. EL spectra were recorded with an EG&G optical multichannel analyzer on a 0.125 m focal length spectrograph, and device brightness is directly measured using a Minolta CS-200 Chroma Meter.

Results and Discussion

Single-Crystal Structure Analysis. PO6 crystallizes in the triclinic space group $P\bar{1}$ with Z = 2 (see Table 1 for a summary and Figure 1 for the thermal ellipsoid plot). The P═O bond lengths [P(1)−O(1) = 1.4867(12) Å and P(2)−O(2) = 1.4844(13) Å] and average P−C bond lengths [1.803 and 1.805 Å, for P(1) and P(2), respectively] are similar about each phosphorus atom and comparable to that reported for Ph_3P═O.[18] However, the molecule is not symmetrical because bond angles about each phosphorus atom are different, exhibiting distorted tetrahedron geometries with O−P−C bond angles averaging 4.9 and 6.1° larger than C−P−C angles, for P(1) and P(2), respectively. The bridging fluorene plane approximately bisects both Ph−P−Ph bond angles [for P(1) = 107.44° and for P(2) = 104.46°], with the P═O groups oriented antiparallel to each other in a transoid conformation relative to the fluorene plane. The oxygen atoms are approximately in-plane with the fluorene

(14) All software and sources of the scattering factors are contained in the SHELXTL (version 5.1) program library. Sheldrick, G. *SHELXTL*, version 5.1; Bruker Analytical X-ray Systems: Madison, WI.
(15) Demas, N. J.; Crosby, G. A. *J. Phys. Chem.* **1971**, *75*, 991.
(16) Klink, S. I.; Hebbink, G. A.; Grave, L.; Oude Alink, P. G. B.; Van Veggel, F. C. J. M.; Werts, M. H. V. *J. Phys. Chem. A.* **2002**, *106*, 3681.
(17) Sapochak, L. S.; Padmaperuma, A.; Washton, N.; Endrino, F.; Schmett, G.; Marshall, J.; Fogarty, D.; Burrows, P. E.; Forrest, S. R. *J. Am. Chem. Soc.* **2001**, *123*, 6300.
(18) Al-Farhan, K. A. *J. Crystallogr. Spectrosc. Res.* **1992**, *22*, 687.

Table 1. Crystal Structure Data for PO6

empirical formula	$C_{39}H_{32}O_2P_2$
fw	594.59
crystal size	0.40 × 0.30 × 0.25 mm^3
crystal system	triclinic
space group	$P\bar{1}$
a	11.200(3) Å
b	11.380(3) Å
c	14.449(4) Å
α	80.357(5)°
β	82.319(4)°
γ	61.405(4)°
volume	1591.2(7) Å^3
Z	2
ρ_{calcd}	1.241 Mg/m^3
2*θ* range	4−58°
F(000)	624
temperature	298(2) K
reflections collected	14 676
independent reflections	7268 [*R*(int) = 0.0259]
wavelength	0.710 73 Å
absorption correction	semiempirical from equivalents
max. and min. transmission	1 and 0.69
refinement method	full-matrix least-squares on F^2
data/restraints/parameters	7268/0/390
goodness of fit on F^2	1.010
final *R* indices [$I > 2\sigma(I)$]	R1 = 0.0425, wR2 = 0.1105
R indices (all data)	R1 = 0.0586, wR2 = 0.1222

perimeter (O−P−C−C torsion angles of 19.95° and 15.35°, for P(1) and P(2), respectively), similar to what has been observed previously for the symmetrical 9,10-bis(diphenylphosphine oxide) anthracene.[19]

In the PO6 crystal, adjacent fluorene units are stacked approximately parallel along the *b* axis, but there are no close $\pi-\pi$ interactions between them (see Figure 2). The molecular packing arrangement observed is dictated, rather, by a balance between strong intermolecular interactions (P−O···H−C and edge-to-face C−H···π contacts) and the longer range electrostatic interactions between P═O moieties. This is not surprising, because the P═O group is a good hydrogen-bond acceptor and phosphine oxides are well-known to form complexes in solution[20] and the solid state.[21] For PO6, each P═O moiety exhibits two close contacts with neighboring molecules via P−O···H−C interactions (see Table 2 and Figure 2a), preventing close $\pi-\pi$ interactions between fluorene bridges. The P═O dipoles lie approximately perpendicular to the *b* axis, forming linear arrays of the type P(2)═O(2)···P(1)═O(1)···P(2)═O(2), alternating between the two independent P═O groups. The extended structure is linked by numerous close contacts via edge-to-face C−H···π interactions (ranging between 2.75 and 2.88 Å) as shown in Figure 2b.

Computational Results. The molecular and electronic structures of PO6 were investigated by computational methods. The gas-phase structure was computed by geometry optimization of the experimental structure obtained from the single-crystal X-ray diffraction data. Similar to the crystal structure, the gas-phase structure showed antiparallel arrangement of polar P═O moieties with the oxygen atoms almost in plane with the fluorene perimeter, minimizing their intramolecular electrostatic interaction. However, the P═O groups are orientated in a *cisoid* conformation with respect to the fluorene plane giving a slightly higher computed net-dipole moment of 2.56 D versus 1.49 D, computed for the experimental structure with the transoid orientation. The difference in total energy between these two structures is calculated to be very small (<3 kJ/mol), indicating that the relative orientation of the antiparallel P═O moieties with respect to the fluorene bridge is dependent on *inter*molecular packing interactions.

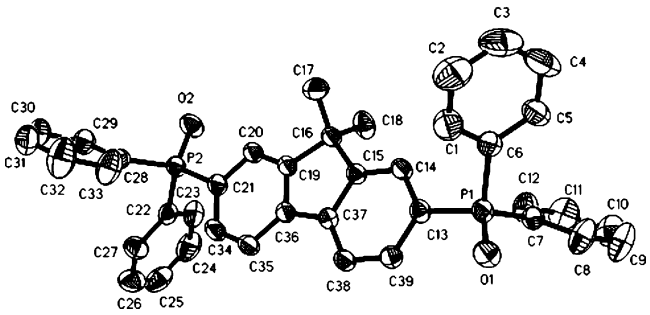

Figure 1. Thermal ellipsoid plot and atomic numbering for PO6.

The orbital amplitude plots for the HOMO and LUMO of PO6 are depicted in Figure 3 and are shown to be localized predominately on the fluorene bridge. The computed HOMO and LUMO energies are not affected by methylation at the 9,9-positions of the fluorene ring nor by the orientation of the P═O moieties with respect to the fluorene bridge. Because the P═O moiety acts as a point of saturation and prevents electronic communication between the fluorene bridge and outer phenyl groups, the photophysics of PO6 are expected to be representative of the fluorene chromophore. However, the strong inductive influence of the polar P═O group is predicted to lower the HOMO and LUMO energies by 0.41 and 0.74 eV, respectively, relative to DMeF. As indicated in Figure 3, the dibromo substitution (BrDMeF) also lowers the HOMO and LUMO energies, but in this case the energy stabilization of the inductive effect is counteracted by a small mesomeric effect.[22]

We also computed the HOMO and LUMO energies for the corresponding diamine, 2,7-diphenylamino-9,9-dimethylfluorene (N6). As expected, the strong electron donating ability of the Ph_2N substitution destabilizes the HOMO by the mesomeric effect and raises the energy significantly compared to DMeF. Because aromatic diamine materials are typically used as hole transport and injection layers in OLED structures, it is instructive to compare how PO6 HOMO and LUMO energies differ from those of N6. As is shown in Figure 3, the PO6 HOMO and LUMO are lower in energy by ∼1.5 eV and ∼0.59 eV, respectively. These theoretical predictions are consistent with similar studies reported by Marsal et al.,[22] for carbazole substituted along the long axis of the molecule with bromo and amino groups.

Photophysical Results. *Electronic Absorption Properties.* The electronic absorption spectrum of PO6 is shown in

(19) Fie, Z.; Kocher, N.; Mohrschladt, C. J.; Ihmels, H.; Stalke, D. *Angew. Chem., Int. Ed.* **2003**, *42*, 783.
(20) Fawcett, J.; Platt, A. W. G.; Russell, D. R. *Inorg. Chim. Acta* **1998**, *274*, 177. Brassat, I.; Englert, W.; Keim, W.; Deitel, D. P.; Killat, S.; Suranna, G.; Wang, R. *Inorg. Chim. Acta* **1998**, *280*, 150.
(21) Calcagno, P.; Kariuki, B. M.; Kitchin, S. J.; Robinson, J. M. A.; Philp, D.; Harris, K. D. M. *Chem.−Eur. J.* **2000**, *6*, 2338 and references therein.
(22) Marsal, P.; Avilov, I.; da Silva Filho, D. A.; Brédas, J. L.; Beljonne, D. *Chem. Phys. Lett.* **2004**, *392*, 521.

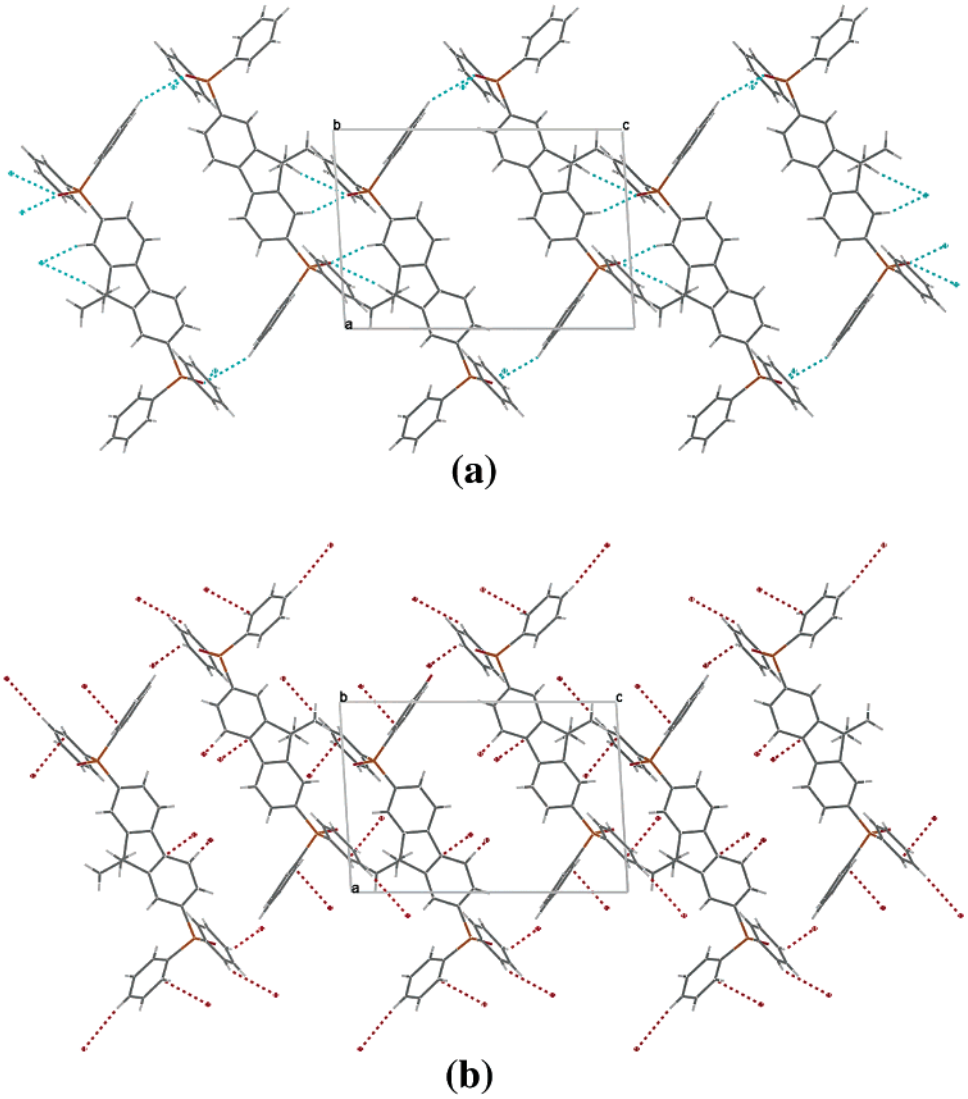

Figure 2. Crystal structure of PO6 viewed along the *b* axis showing (a) short P−O···H−C contacts indicated by cyan dashed lines and (b) short C−H···π contacts indicated by red dashed lines.

Table 2. Close Contacts Due to P−O···H−C Interactions in the PO6 Crystal

interaction	C···O (Å)	C−H···O (deg)
P(1)−O(1)−H(25)−C(25)	3.48	154.2
P(1)−O(1)−H(38)−C(38)	3.26	140.7
P(2)−O(2)−H(18C)−C(18)	3.47	163.6
P(2)−O(2)−H(20)−C(20)	3.53	157.9

Figure 4 and is compared to the corresponding spectra for fluorene and BrDMeF. The electronic transitions in fluorene have previously been assigned according to the symmetry elements of the molecule.[23] For PO6, substitution at the 2,7-positions by diphenylphosphine oxide ($Ph_2P{=}O$) strongly polarizes the long axis of the molecule without increasing the electron delocalization length of the active chromophore, in contrast to the diphenyl amino derivative reported previously.[24] As a consequence, PO6 exhibits a well-defined absorption spectrum similar to fluorene with increased molar absorptivity (by ∼4−14 times) and small red shift of all bands (by ∼1500−2200 cm^{-1}; see Figure 4) whereas the absorption of the diphenyl amino derivative is broadened and red-shifted by >6000 cm^{-1}.[24] The smaller red shift observed for BrDMeF is likely because of a small counteractive mesomeric effect consistent with our computational predictions.

Photoluminescence (PL) Properties. The fluorescence and phosphorescence spectra of PO6 and BrDMeF are shown in Figure 5. PO6 exhibits very strong and structured UV emission peaking at 335 nm with a small Stoke's shift (1895 cm^{-1}) and high fluorescence QE ($\phi_s = 0.98$, $\tau_s = 1.02$ ns). The emission spectrum of PO6 is similar to that of BrDMeF but exhibits better defined vibrational fine structure (see Figure 5). These photophysical properties are characteristic of the fluorene chromophore which emits at 312 nm in CH_2Cl_2 with a small Stoke's shift (1780 cm^{-1}).

Phosphorescence spectra of PO6 and BrDMeF were obtained in CH_2Cl_2 at 77 K and are also shown in Figure 5. Previously, the triplet energies (E_T) of fluorene and DMeF were reported to be 2.94 eV[25] and 2.92 eV,[26] respectively,

(23) Dick, B.; Hohlneicher, G. *Chem. Phys.* **1985**, *94*, 131.
(24) Belfield, K. D.; Bondar, M. V.; Przhonska, O. V.; Schafer, K. J.; Mourad, W. *J. Lumin.* **2002**, *97*, 141.
(25) Palmer, T. F.; Parmar, S. S. *J. Photochem.* **1985**, *31*, 273.
(26) Davydov, S. N.; Rodionov, A. N.; Shigorin, D. N.; Syutkina, O. P.; Krasnova, T. L. *Russ. J. Phys. Chem.* **1981**, *55*, 444.

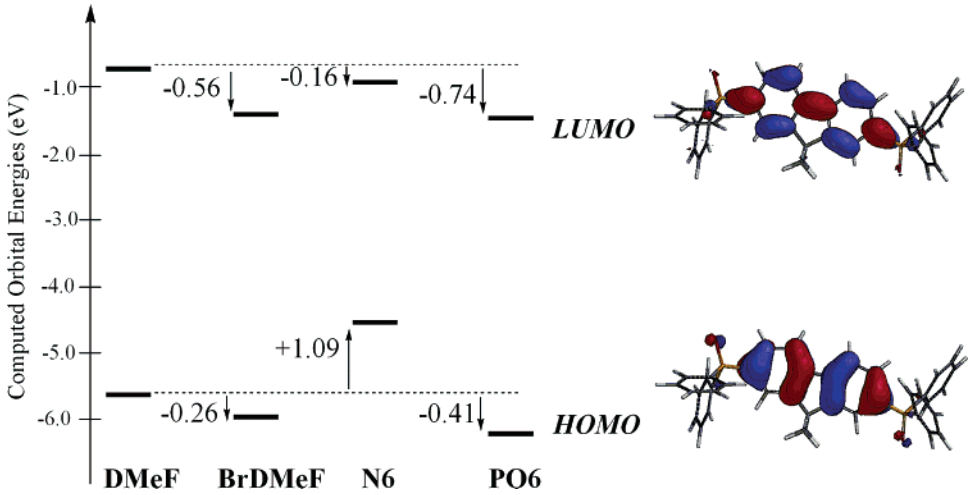

Figure 3. Comparison of the change in computed HOMO and LUMO energies (B3LYP/6-31G*) caused by 2,7-disubstitution of the DMeF bridge with bromo (BrDMeF), diphenylamino (N6), and diphenylphosphine oxide (PO6). The orbital amplitude plots of the HOMO and LUMO are shown for PO6.

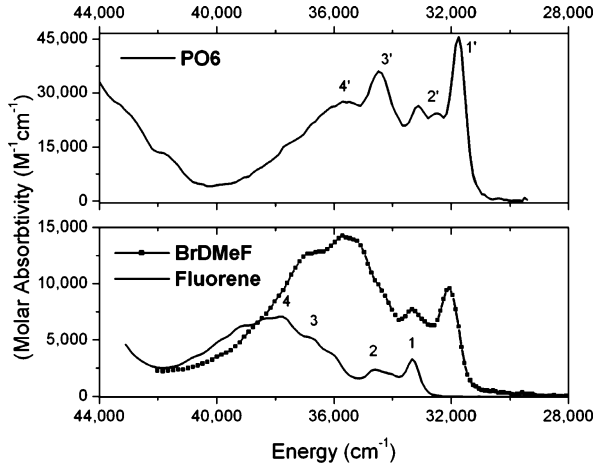

Figure 4. Comparison of the electronic absorption spectra in CH_2Cl_2 for PO6, fluorene, and 2,7-dibromo-9,9-dimethylfluorene (BrDMeF). Major absorption bands are labeled according to assignments reported for fluorene previously.[23]

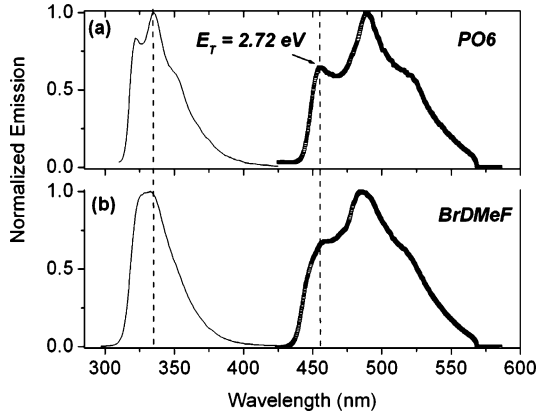

Figure 5. PL spectra for (a) PO6 and (b) BrDMeF in CH_2Cl_2 at room temperature showing fluorescence (thin lines) and at 77 K with detector delay showing phosphorescence (thick lines). The triplet energy (E_T) is indicated and identified as the highest energy peak ($\nu_{0,0}$) in the phosphorescence spectra.

as determined from the $\nu_{0,0}$ transitions identified as the highest-energy band of their phosphorescence spectra. Here, PO6 and BrDMeF exhibit phosphorescence peaks at 489 and 485 nm, respectively, but have similar $\nu_{0,0}$ peaks at 455 nm corresponding to a $E_T \sim 2.72$ eV. Triplet energies are lowered by ~0.2 eV compared to fluorene mainly through the aforementioned inductive effects, which are similar for both $Ph_2P{=}O$ and Br substitution. In the case of the latter, the energy lowering of E_T is similar to what has been predicted[22] and observed[27] previously for brominated carbazole derivatives.

The absorption and fluorescence spectra of PO6 showed no dependence on solvent polarity. However, as the solution concentration increased ($>10^{-5}$ M, CH_2Cl_2), significant self-absorption on the high-energy side of the emission peak and a new, structured low energy emission with two discernible peaks at 376 and 397 nm were observed (see Figure 6a). Similar effects were not observed for concentrated solutions of fluorene or BrDMeF in CH_2Cl_2. Although we note that low energy emission centered at 370 nm, attributed to excimer emission,[28] has previously been reported for fluorene at low temperatures, such emission is usually broad and unstructured. The source of the structured, low energy emission observed for PO6 at room temperature is more likely due to ground-state aggregates, because it is common for phosphine oxides to form extended structures in solution and the solid state through strong P−O···H−C and C−H···π intermolecular interactions,[21] as are present in PO6. No meaningful absorption data at high solution concentration could be collected because of the high extinction coefficient of the UV peaks, but results from solid-state samples are supportive of aggregate emission as discussed below.

Solid-state film samples (300 and 1450 Å thick) formed by thermal vapor deposition exhibited absorption spectra similar to those of a dilute solution. However, the emission spectra were similar to those obtained from concentrated solutions but with weaker UV emission ($\lambda_{max} = 339$ nm) and more prominent low energy emission with peaks at 378 and 397 nm (see Figure 6b). The film emission spectra were independent of excitation energy, and the excitation spectra of the 339 and 397 nm peaks were identical, suggesting that both emission peaks originate from the same ground-state species. We propose that the structured low energy emission

(27) Brunner, K.; van Dijken, A.; Borner, H.; Bastiaansen, J. J. A. M.; Kiggen, N. M. M.; Langeveld, B. M. W. *J. Am. Chem. Soc.* **2004**, *126*, 6035.
(28) Harrocks, D. L.; Brown, W. G. *Chem. Phys. Lett.* **1970**, *5*, 117.

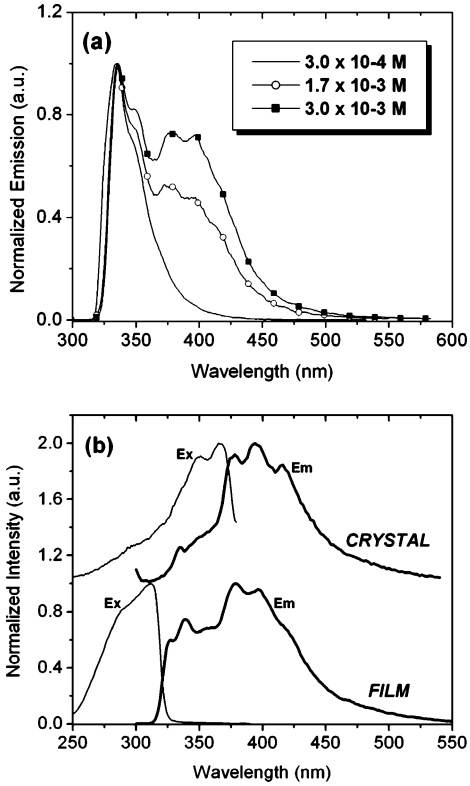

Figure 6. (a) PL spectra for PO6 at different concentrations in CH_2Cl_2. (b) Comparison of excitation (λ_{em} at 400 nm) and emission spectra for PO6 in the solid-state film (300 Å thick) and crystalline solid.

in the thin films is more likely from a low density of crystalline aggregates than from excimers. This supposition is strengthened by the observation of (1) predominately low energy emission from a crystal of PO6 placed in a quartz capillary (and crystalline solid pressed onto a quartz slide) and (2) a new band responsible for this emission seen in the excitation spectra (see Figure 6b). In the crystal structure of PO6, although the fluorene units stack parallel, no close $\pi-\pi$ interactions ($\leq$3.5 Å) of the fluorene chromophores occurs but strong P−O···H−C and C−H···π intermolecular interactions dominate and likely induce aggregate formation at high concentrations in solution and in the solid-state film. On the basis of these results, we propose that a very small density of aggregates is responsible for the low energy emission, which are, therefore, not visible in the excitation spectrum of the film (no new absorption bands and no observable evidence of crystallization) but are revealed in the PL spectrum (by energy transfer to the lower energy sites).

EL Results. A simple bilayer electroluminescent device was made consisting of a 20 nm thick layer of CuPc on ITO coated glass followed by a 30 nm thick layer of PO6 capped with a cathode. Structured UV emission (335 nm) and low energy emission with two distinct peaks (380 and 397 nm) were observed in the EL spectrum, which was similar to the PL spectrum of the vapor deposited film (see Figure 7). The external QE (η_{ex}) was 0.01% (corrected for glass/ITO/CuPc absorption, as described previously),[9] and the operating voltage was 3.4 V at a 13 mA/cm^2 drive current. The low η_{ex} and low drive voltage is consistent with electron transport in PO6 but limited hole injection from CuPc into PO6 and no effective electron confinement, as discussed previously for similar devices incorporating 4,4′-bis(diphenylphosphine

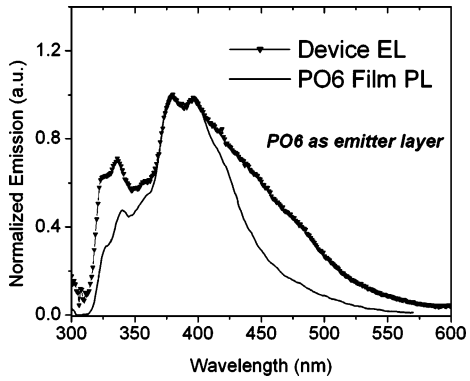

Figure 7. EL spectra from ITO/CuPc/PO6/LiF−Al device compared to the PL spectrum of a 300 Å thick vapor deposited film of PO6.

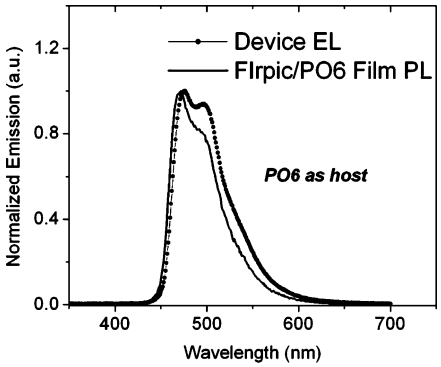

Figure 8. Normalized spectra of EL from ITO/CuPc/NPD/TCTA/10% FIrpic:PO1/PO1/LiF−Al device and of PL from coevaporated film of 10% FIrpic in PO6 grown on quartz.

oxide)biphenyl (PO1).[9] In both cases, the organic phosphine oxide materials are predicted to have significantly deeper HOMO energies compared to typical diamine materials used for hole injection and transport but have accessible LUMO levels for facile electron injection and transport.[9] We, therefore, conclude that PO6 functions as an electron transporting material in an OLED configuration.

To demonstrate the use of PO6 as a host material for blue electrophosphorescence, devices were made using the shortest wavelength commercially available phosphorescent dopant, FIrpic doped at 5, 10, and 20% by mass. The device structure was ITO/CuPc(20 nm)/α-NPD(20 nm)/TCTA(6 nm)/5−20%FIrpic:PO6(20 nm)/PO6(20 nm)/LiF(1 nm)/Al(100 nm). At dopant concentrations $\geq$ 5% only FIrpic emission is observed in the EL spectra indicating complete energy transfer to the phosphorescent dopant with no measurable spectral effects due to PO6 aggregates (see Figure 8).

The external QE (η_{ex}) and luminous power efficiency (η_p) of this series of devices are depicted in Figure 9a, and all device results are summarized in Table 3. Using 10% FIrpic in PO6, we obtain a maximum QE of 8.1% at 2 μA/cm^2 and 3 V. As the drive current is increased to a brightness of 800 cd/m^2 the η_{ex} drops to 4.4% at 5.6 V. These data correspond to efficiencies of 21.5 cd/A and 11.8 cd/A, respectively. Assuming approximately Lambertian emission into π steradians, the corresponding derived luminous power efficiencies are 25.1 lm/W and 6.7 lm/W, respectively.[29] We note that the triplet energies of PO6 and FIrpic are similar (both $\sim$

(29) Forrest, S. R.; Bradley, D. C. C.; Thompson, M. E. *Adv. Mater.* **2003**, *15*, 1043.

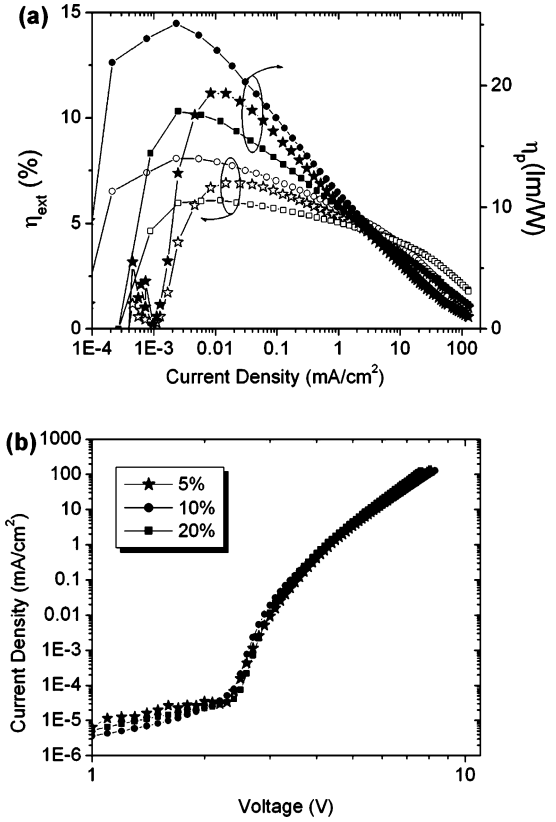

Figure 9. (a) Comparison of the external quantum efficiencies (open symbols) and luminous power efficiencies (solid symbols) for device structure: ITO/20 nm CuPc/20 nm NPD/6 nm TCTA/(20 nm) (*X*% FIrpic: PO6)/20 nm PO6/LiF−Al, with *X*% = 5 (star), 10 (circle), and 20 (square), and (b) current density vs voltage plots for each device.

Table 3. Device Properties[a] for Different Percentages of FIrpic Doped into PO6

property	5%	10%	20%
$\eta_{ex,max}$ (%) [J (mA/cm^2)]	6.9 (0.015)	8.1 (0.002)	6.1 (0.012)
$\eta_{c,max}$ (cd/A)	18.5	21.5	16.3
$V_{opt@max\ QE}$	3.0	3.0	2.8
$\eta_{p,max}$ (lm/W) [J (mA/cm^2)]	19.4 (0.015)	25.1 (0.002)	17.9 (0.002)
$\eta_{ex}{}^b$ (%)	4.1	4.4	4.3
J^b (mA/cm^2)	6.3	7.6	7.3
$\eta_c{}^b$ (cd/A)	10.9	11.8	11.4
$V_{opt}{}^b$	5.4	5.6	5.3
$\eta_p{}^b$ (lm/W)	6.3	6.7	6.8

[a] $\eta_{ex,max}$, maximum external QE; $\eta_{c,max}$, maximum luminance efficiency; $\eta_{p,max}$, maximum luminance power efficiency; and V_{opt}, operating voltage at a specified current. [b] Reported at lighting brightness (800 cd/m^2).

2.7 eV), which may result in incomplete energy transfer to the phosphor. Indeed, the measured device quantum efficiencies are slightly lower than those of the best devices obtained using carbazole-based host materials.[7,30] The significantly reduced operating voltage of PO6 devices and decreased dependence on the dopant molecule concentration (see Figure 9b and Table 3) nonetheless offer the potential for higher *power* efficiency devices. We ascribe the lower operating voltage to efficient electron injection and transport in PO6 (hole injection and transport likely occurs on FIrpic molecules because of the deep HOMO energy of PO6).

We have not performed lifetime testing on devices appropriately encapsulated for long operating lifetimes. Devices using 4,4′-bis(diphenylphosphine oxide)biphenyl (PO1) as the host material showed visible crystallization and significantly reduced QE after 24 h of storage in N_2.[9] In the case of PO6, replacement of the biphenyl bridging moiety with the more rigid fluorene unit increased the glass transition temperature by ∼15 °C, but crystalline aggregate emission was still observed from film samples and device lifetimes were similarly short. Because triaryl phosphine oxides are known to exhibit high chemical and thermal (pyrolysis) stabilities,[31,32] we believe device lifetimes are limited by crystallization. The presence of highly polar P═O moieties coupled with small rotational barriers about the P−aryl bonds creates a high propensity for crystallization in both PO1 and PO6 which we expect will be reduced via substitution of more bulky outer group structures and is the subject of future work.

Conclusions

The synthesis and characterization of a new fluorene derivative (PO6) substituted along the long axis of the molecule (2,7-positions) with diphenylphosphine oxide groups is reported. The P═O moieties are used as points of saturation to electronically isolate the fluorene bridge from the outer phenyl groups allowing the photophysical properties of volatile moieties such as DMeF to be incorporated into a vacuum sublimable material. Even though PO6 exhibits low energy emission similar to other fluorene oligomers and polymers, the emission energy is high enough not to interfere in its ability to serve as a host for short wavelength dopants, such as FIrpic. The low device operating voltages using PO6 as a host material for blue electrophosphorescence are likely a result of a low LUMO energy favorable to electron injection coupled with partial solid state ordering driven by the strong intermolecular interactions through P−O···H−C and C−H···π close contacts identified in the crystal. The hole transporting properties of PO6 were not determined due to the difficulty of injecting holes into the low-lying HOMO level. The results suggest that phosphine oxide moieties may be used to construct materials amenable to vacuum sublimation from small, volatile, high triplet state energy building blocks such as fluorene.

Acknowledgment. We acknowledge financial support from the U.S. Department of Energy/Building Technologies Solid-State Lighting Program. We also would like to thank Dr. A. Joly (photophysics) and Dr. S. Burton (NMR) from the Environmental Molecular Sciences Laboratory (EMSL), Dr. P. Vecchi (PNNL) and Dr. A. Ellern (Molecular Structure Laboratory, Iowa State University) for X-ray crystallography, and Dr. K. Ferris (computational support). Pacific Northwest National Laboratory (PNNL) is operated by Battelle Memorial Institute for the U.S. Department of Energy (DOE) under Contract No. DE-AC06-76RLO 1830.

Supporting Information Available: The X-ray structural information (CIF) and crystal structure data (PDF). This material is available free of charge via the Internet at http://pubs.acs.org.

CM0600677

(30) Yeh, S.-J.; Wu, M.-F.; Chen, C.-T.; Song, Y.-H.; Chi, Y.; Ho, M.-H.; Hsu, S.-F.; Chen, C. H. *Adv. Mater.* **2005**, *17*, 285.

(31) Berlin, K. D. Butler, G. B. *Chem. Rev.* **1960**, *60*, 243.

(32) Bailey, W. J.; Muir, W. M.; Marktscheffel, R. *J. Org. Chem.* **1962**, *27*, 4404.